Proceedings of the 26th Annual International Conference of the IEEE EMBS
San Francisco, CA, USA • September 1-5, 2004

Bias Voltages at Microelectrodes Change Neural Interface Properties *in vivo*

M. D. Johnson[1], K. J. Otto[1], J. C. Williams[2], D. R. Kipke[1]
[1]Department of Biomedical Engineering, University of Michigan, MI, USA
[2]Department of Biomedical Engineering, University of Wisconsin-Madison, WI, USA

Abstract—**Rejuvenation of iridium microelectrode sites, which involves applying a 1.5 V bias for 4 s, has been shown to reduce site impedances of chronically implanted microelectrode arrays. This study applied complex impedance spectroscopy measurements to an equivalent circuit model of the electrode-tissue interface. Rejuvenation was found to cause a transient increase in electrode conductivity through an IrO_2 layer and a decrease in the surrounding extracellular resistance by 85 ± 1% (n=73, t-test p<0.001) and a decrease in the immediate site resistance by 44 ± 7% (n=73, t-test p<0.001). These findings may be useful as an intervention strategy to prolong the lifetime of chronic microelectrode implants for neuroprostheses.**

Keywords—**bias voltage, microelectrodes, neural interface, neuroprostheses, rejuvenation**

I. Introduction

Developing intervention strategies to limit the extent of tissue reaction at microelectrode sites is important for extending the functional longevity of chronically implanted microelectrode arrays. Passing current through a neural iridium microelectrode *in vivo* has been shown to cause a reduced 1 kHz site impedance and improvement in unit recordings [1, 2]. However, the underlying mechanisms for this drop in impedance are not fully known. In this study, we investigated how bias voltages (rejuvenation) affect iridium microelectrode characteristics as well as the surrounding neural tissue through an equivalent circuit model.

II. Methodology

A. Device and Surgical Implantation

Seven male Sprague-Dawley rats (250-300g) were chronically implanted with Michigan silicon microelectrode arrays as described elsewhere [3, 4]. A period of at least 3 weeks was allotted for each rat before starting the rejuvenation experiments. This allowed for the typical tissue reactive response to peak and settle [5]. Briefly, the arrays consisted of four 50 μm-wide thin-film silicon shanks separated by 200 μm. Each shank had four iridium microelectrodes (703 μm^2) with 200 μm spacings. In two of the rats, an activated iridium array was surgically implanted in the auditory cortex [6] and an unactivated array was inserted in the forelimb region of the rat's primary motor cortex [7]. The other five rats were implanted with two arrays in the forelimb region. All procedures complied with the guidelines for the care and use of laboratory animals and were approved by the University of Michigan Committee on Use and Care of Animals.

B. Electrochemical Methods

Electrochemical measurements were made with an Autolab PGSTAT12 (Eco Chemie, Netherlands). Iridium microelectrode arrays functioned as the working electrodes with bone screws (stainless steel 316SS) serving as reference and counter electrodes. The 316SS grade was chosen since it provides a stable reference *in vivo* [8].

The auditory arrays were activated with hydrous oxide layers ($Ir(OH)_3$) in a well-characterized charge injection method that involved applying a 1 Hz square wave (-0.85 V to 1 V) for >100 s [9, 10]. The primary rejuvenation procedure employed in this study was biasing an electrode site with 1.5 V for 4 s with currents limited to <300 nA.

Two potentiostatic methods – electrochemical impedance spectroscopy (EIS) and cyclic voltammetry (CV) – facilitated the analysis of changing electrode and tissue characteristics. EIS involved applying a 25 mV rms sine wave (100 Hz to 10 kHz). CV used a linear sweeping voltage from -0.5 to 1 V with a 1 V/s scan rate. Both types of measurements were made prior to and immediately after rejuvenation sessions for all rats, and in two cases, for a period of 10 days.

C. Neural Interface Model (NIM)

An equivalent circuit model for the electrode-tissue interface has been developed previously (see Fig. 1) and shown to delineate tissue reaction changes at a microwire electrode after chronic implantation [11, 12]. The model algorithm took complex impedance spectroscopy measurements and estimated circuit components by iteratively fitting the high and low-frequency data points to their respective circuit pathways. Parameter estimations that did not fit a 0.95 r^2 measure were discarded.

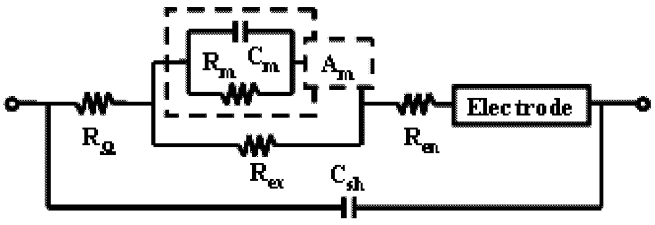

Fig. 1. Equivalent circuit model of the iridium microelectrode and surrounding neural tissue.

The electrode component of the neural interface model (NIM) was modeled with a constant phase element (CPE), described by Eq. 1 with a gain term (K) and a phase term (α). A CPE was sufficient to describe the non-ideal double-layer capacitance behavior [13]. Activated iridium electrodes were modeled with an additional capacitance (C_{ox}) in parallel to the CPE and a resistance (R_{ox}) as demonstrated by Weiland et al [8].

$$Z_{CPE} = \frac{K}{(j\omega)^{\alpha}}. \quad (1)$$

Neural tissue in the immediate vicinity of the microelectrode was modeled with a nearby encapsulation resistance (R_{en}), a more distant extracellular resistance (R_{ex}), and a cellular circuit [14], involving membrane capacitance (C_m=1x10^{-6} μF/cm^2), membrane resistance (R_m=0.3 S/cm^2), and a scaling factor term (A_m). The spreading resistance at the counter electrode was given by R_Ω.

III. Results

A. Rejuvenation Effects on Site Impedances

The following results are from one rat, implanted with an auditory and a motor microelectrode array (16 sites each), unless stated otherwise. Rejuvenation-induced changes in the electrode-tissue interface were consistent among all seven rats.

To determine how rejuvenation intensity affected the 1 kHz site impedances, electrodes were stepped in 0.25 V increments (see Fig. 2). For such arrays, site impedances tended to fall-off near a 0.75 V bias potential and reached a minimum at a 1.5 V potential. Although not shown graphically, applying a 1.75 V bias did not cause a significant decrease in site impedance. For the entire array, site impedances began at 2.4 ± 0.039 MΩ and ended at 574 ± 1.3 kΩ after rejuvenation (n=16, t-test p<0.0001). Stepping the bias voltage back to 0 V and beyond to -0.75 V did not produce a significant increase in impedance suggesting that rejuvenation caused a lasting change in the electrode-tissue interface.

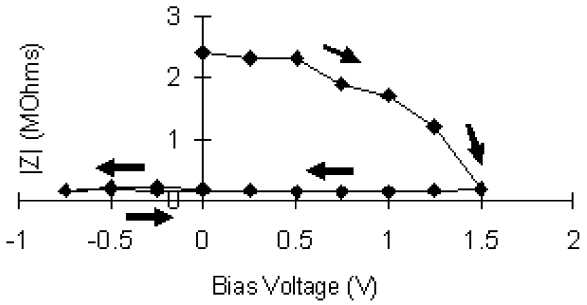

Fig. 2. 1kHz site impedances after bias voltage.

The four-second duration of the anodic bias had been explored previously and shown effective at improving unit recordings [15]. Variations in rejuvenation durations from 2 to 5 s produced charge injections from 9.2 to 350 nC, which did not correlate with changes in 1kHz impedances. In order to determine whether the impedance drops resulted from an impedance reduction in the electrode, in the tissue, or in a combination, additional microelectrode arrays were rejuvenated in PBS 0.1X.

B. Rejuvenation Effects on Iridium

In vitro rejuvenation of native iridium microelectrodes caused a drop in the 1 kHz impedance from 1.113 ± 0.064 MΩ to 637 ± 15 kΩ (n=10, t-test p<0.001). In contrast, previously activated iridium electrodes (~30 mC/cm^2) did not show a significant 1 kHz impedance drop.

Another means for determining rejuvenation effects on iridium involved analyzing cyclic voltammetry curves acquired before and after rejuvenation. For the *in vitro*

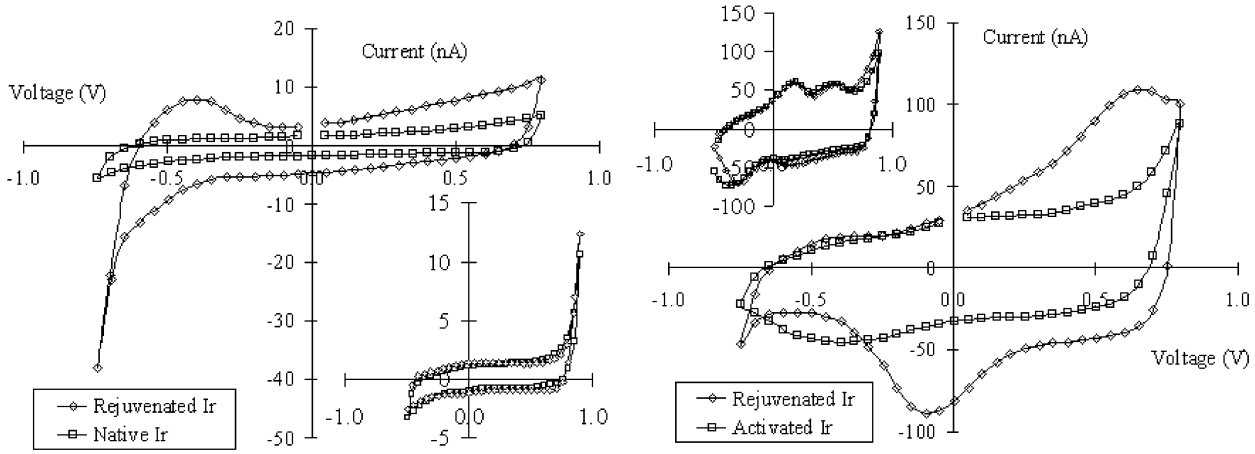

Fig. 3. Cyclic voltammetry curves: (A) average of 16 native iridium sites before and after rejuvenation *in vivo* (inset: *in vitro*). (B) average of 16 activated sites before and after rejuvenation *in vivo* (inset: *in vitro*).

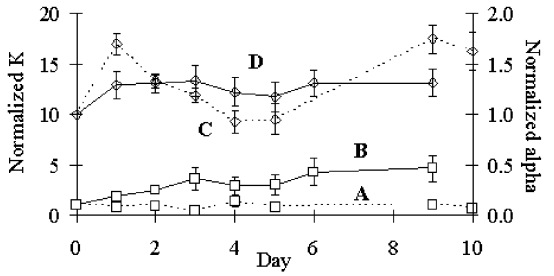

Fig. 4. Normalized electrode gain K for activated (A, n=12) and native (B, n=6) iridium. Normalized electrode phase α for activated (C, n=12) and native (D, n=6) iridium.

iridium electrodes, the CV curves did not seem to have any significant waveform changes after rejuvenation, which was not the case for the *in vivo* iridium electrodes (see Fig. 3). Following rejuvenation native iridium charge storage capacity (Qcap) increased from 1.01 ± 0.36 mC/cm^2 to 3.20 ± 0.07 mC/cm^2 (n=16, t-test, p<0.001), and from 17.12 ± 0.36 mC/cm^2 to 25.73 ± 0.48 mC/cm^2 (n=13, t-test, p<0.001) for previously activated iridium electrodes.

A third method for determining changes in iridium properties involved estimating constant phase element parameters K (the electrode gain) and α (electrode phase) through EIS measurements. Stepping rejuvenation voltages by 0.25 V demonstrated that α remained constant until 1.5 V whereby it increased significantly (t-test, p<0.001); on the other hand, K decreased linearly with each 0.25 V step. Fig. 4 shows that the phase terms increased for both native and activated iridium *in vivo* suggesting that rejuvenation may 'clean' the electrode surface. The observation that K increased for the native iridium over the 10 day period was not found to be consistent with other rats observed long-term.

C. Rejuvenation Effects on Neural Tissue

Through our iterative algorithm, components in the Neural Interface Model were estimated from the complex impedance spectroscopy data before and after rejuvenation. The two cellular tissue components (R_{ex} and A_m) both changed dramatically after rejuvenation. The normalized value of R_{ex} for rejuvenated sites decreased by 86 ± 1% (n=73, t-test, p<0.001), while the normalized value of R_{ex} for adjacent non-rejuvenated sites increased by a negligible 5 ± 7% (n=18, t-test, p=0.508). The normalized values for A_m on rejuvenated sites increased by 954 ± 75% (n=73, t-test, p<0.001) with adjacent non-rejuvenated sites increasing by only 14 ± 8% (n=18, t-test, p=0.644). In contrast to the tissue components, the values for encapsulation resistance R_{en} decreased both for rejuvenated sites by 44 ± 7% (n=73, t-test, p<0.001) and for non-rejuvenated sites 31 ± 5% (n=18, t-test, p<0.001).

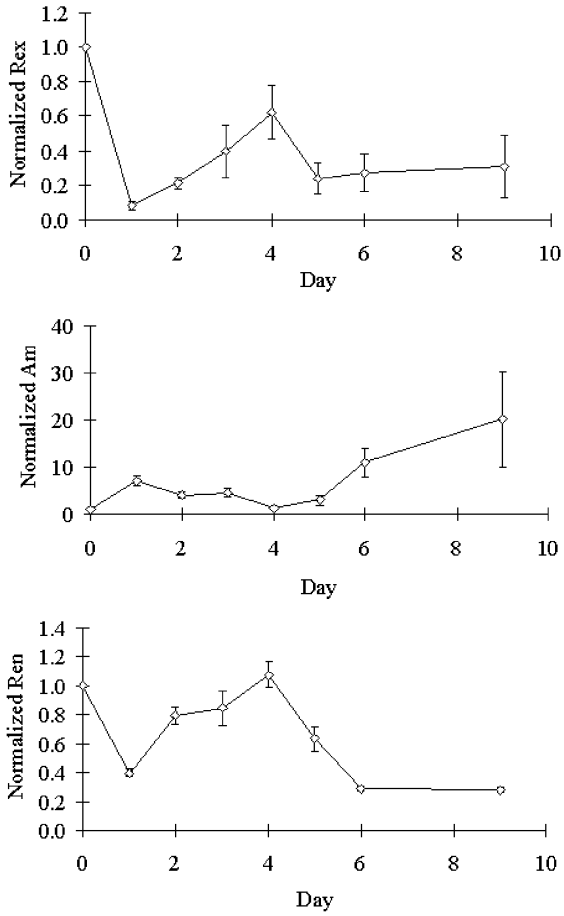

Fig. 5. (1) Normalized encapsulation resistance R_{en} for native iridium. (2) Normalized cellular scaling factor A_m for native iridium. (3) Normalized extracellular resistance R_{ex} for native iridium.

The model was extended to complex impedance data sets over a period of ten days to determine the lasting effects of rejuvenation on neural interface parameters (see Fig. 5). Again, R_{ex} and A_m showed an inverse relationship, while R_{en} was more variable. At day 4, both arrays saw a significant increase in R_{ex} with a decrease in A_m, followed by a return to the post-rejuvenation levels (day 1).

IV. Discussion

The results indicate that rejuvenation causes a significant drop in 1kHz site impedances and that the changes originate from both increasing iridium electrode conductivity and decreased neural tissue resistance.

Increased charge capacities and altered waveform shapes are thought to represent the formation of an inner IrO_2 layer, consistent with the initial anodic bias during activation. However, it was observed that the increased charge capacity

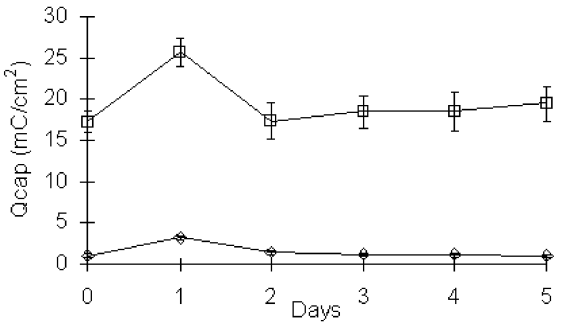

Fig. 6. Charge capacity (Qcap) for the native (lower trace, n=16) and activated (upper trace, n=13) iridium electrodes before (day 0) and after rejuvenation (day 1 to 5).

was transient. Between the 2nd and 4th days post-rejuvenation, CV waveforms returned to their pre-rejuvenation levels for both native and activated iridium, indicating that that the inner charge layer was not stable *in vivo* (see Fig. 6).

According to the model, neural tissue resistances decreased significantly post-rejuvenation. The scaling factor A_m and extracellular resistance R_{ex} were found to be inversely related. In addition, changes in all neural tissue parameters R_{en}, R_{ex}, and A_m peaked at 4-7 days, which may be caused by a resetting of the host response to the foreign microelectrode array in the brain [5].

Varying the rejuvenation durations resulted in a range of charge injections. Tissue components, however, did not correlate with the amount of charge injected, which may suggest that even small amounts of charge injection can be beneficial to decrease tissue impedances. Future studies will examine correlations between the neural interface model parameters and both unit recordings and histology.

V. Conclusion

This study investigated the underlying mechanisms of rejuvenation through an equivalent circuit model of the neural interface. Rejuvenation involved passing a small amount of current (typically 200 nA) over 4 s with a 1.5 V DC bias between an iridium microelectrode site and a 316SS reference bone screw. Our findings indicate that rejuvenation caused a temporary enhancement to the electrode oxide conduction and a more substantial long-term change in the resistance of the encapsulated and extracellular spaces surrounding the microelectrode. This technique may be a useful intervention strategy to prolong the functional lifetime of chronically implanted microelectrode arrays.

Acknowledgment

The authors would like to thank the Neural Engineering Laboratory. Probes were fabricated and assembled through the Center for Neural Communication Technology (CNCT) sponsored by NIH NIBIB grant P41-EB002030-11. This work was supported by the CNCT and the Engineering Research Centers program of the National Science Foundation under NSF Award Number EEC-9986866.

References

[1] K. Wise, "Neural Prosthesis Program QPR2 - "Chronic Implantation of Passive Probes"," January-March 1991.

[2] E. Schmidt, "Chronic Neural Recording with Multi-contact Silicon Microprobes: Effects of Electrode Bias," presented at Abstracts of the 24th Annual Meeting of the Society for Neuroscience, Miami Beach, 1994.

[3] D. R. Kipke, R. J. Vetter, J. C. Williams, and J. F. Hetke, "Silicon-substrate intracortical microelectrode arrays for long-term recording of neuronal spike activity in cerebral cortex," *Ieee Transactions on Neural Systems and Rehabilitation Engineering*, vol. 11, pp. 151-155, 2003.

[4] R. J. Vetter, et al, "Chronic neural recording using silicon-substrate microelectrode arrays implanted in cerebral cortex," *IEEE Trans Biomed Eng*, In Press.

[5] J. N. Turner, W. Shain, D. H. Szarowski, M. Andersen, S. Martins, M. Isaacson, and H. Craighead, "Cerebral astrocyte response to micromachined silicon implants," *Exp Neurol*, vol. 156, pp. 33-49, 1999.

[6] S. L. Sally and J. B. Kelly, "Organization of auditory cortex in the albino rat: sound frequency," *J Neurophysiol*, vol. 59, pp. 1627-38, 1988.

[7] J. N. Sanes, S. Suner, and J. P. Donoghue, "Dynamic organization of primary motor cortex output to target muscles in adult rats. I. Long-term patterns of reorganization following motor or mixed peripheral nerve lesions," *Exp Brain Res*, vol. 79, pp. 479-91, 1990.

[8] J. D. Weiland and D. J. Anderson, "Chronic neural stimulation with thin-film, iridium oxide electrodes," *IEEE Trans Biomed Eng*, vol. 47, pp. 911-8, 2000.

[9] L. S. Robblee, J. L. Lefko, and S. B. Brummer, "Activated Ir - an Electrode Suitable for Reversible Charge Injection in Saline Solution," *Journal of the Electrochemical Society*, vol. 130, pp. 731-733, 1983.

[10] R. D. Meyer, S. E. Cogan, T. H. Nguyen, and R. D. Rauh, "Electrodeposited iridium oxide for neural stimulation and recording electrodes," *Ieee Transactions on Neural Systems and Rehabilitation Engineering*, vol. 9, pp. 2-11, 2001.

[11] J. C. Williams, D. R. Kipke, G. D. Smith, and W. Shain, "Modeling the complex electrical impedance spectral properties of the electrode-tissue interface," presented at Neural Prosthesis Workshop, Bethesda, MD, 2001.

[12] J. C. Williams, "Ph.D. Dissertation: "Performance of Chronic Neural Implants"." Tempe, AZ: Arizona State University, 2001.

[13] E. T. Mcadams, A. Lackermeier, J. A. Mclaughlin, D. Macken, and J. Jossinet, "The Linear and Nonlinear Electrical-Properties of the Electrode-Electrolyte Interface," *Biosensors & Bioelectronics*, vol. 10, pp. 67-74, 1995.

[14] J. R. Buitenweg, W. L. Rutten, W. P. Willems, and J. W. van Nieuwkasteele, "Measurement of sealing resistance of cell-electrode interfaces in neuronal cultures using impedance spectroscopy," *Med Biol Eng Comput*, vol. 36, pp. 630-7, 1998.

[15] W. Heetderks and E. Schmidt, "Personal Communication," 1997.